DALTON

The chemistry and the geometric and electronic structures of small naked metal clusters prepared using a rotating cryostat and studied by electron paramagnetic resonance †

Brynmor Mile,*[a] Philip D. Sillman,[b] Abdul R. Yacob[b] and James A. Howard[c]

[a] *The School of Chemistry, University of Bristol, Cantock's Close, Bristol BS8 1TS, UK*
[b] *Department of Chemistry, University of Wales Cardiff, PO Box 912, Cardiff CF1 3TB, UK*
[c] *Steacie Institute for Molecular Sciences, N.R.C.C. Ottawa, Ontario K1A OR9, Canada*

A rotating cryostat has been used to generate several new naked metal clusters whose structures and reactions have been studied by EPR spectroscopy. Most alkali-metal trimers adopt an obtuse triangular geometry with a $^2B_2$ ground state in C_{2v} symmetry. A new acute Na_3 cluster was formed by interaction with water, $Na_3(H_2O)_x$ where $x \geqslant 1$. The first EPR spectrum of a mixed alkali-metal trimer, Na_2Li, has been recorded. The fluxionality of both Na_3 and Li_3 in an adamantane matrix is lost and a static form results with the Li located at the apical position. The first ENDOR (electron nuclear double resonance) spectrum of a naked metal cluster, Li_3, has been recorded. It gives more accurate paramagnetic parameters and shows conclusively that the cluster is a fluxional, pseudo-rotating Jahn–Teller molecule. The ENDOR spectra of $Li_3(H_2O)_x$ complexes were also observed. A new coinage metal trimer, Au_2Ag, has been characterised by EPR spectroscopy and has the silver in the apical position in a static obtuse structure. Reactions of the alkali-metal and coinage-metal trimers with simple molecules such as water and ethene resulted in a change in geometry from an obtuse or fluxional molecule to an acute static entity. The flexible nature of clusters is discussed in the context of modelling the chemical events occurring at the active metallic sites of heterogeneous catalysts.

The launching of this first Dalton Discussion on the theme of metal clusters is in itself attestation that research in this field is flourishing and important. Metal clusters lie between the extremes of the isolated atom and the bulk metal and are therefore of fundamental interest to anyone concerned with the nature of matter as understood in terms of quantum theory. They provide a natural meeting place for physicists, especially the solid-state variety, and chemists.

They are of commercial importance since their exhibition of quantum-size effects may well prove important in the development of new quantum-dot, -well and -line devices.[1] They are the nuclei for phase changes and are also the latent image in the silver halide photographic process. They provide useful, informative models for describing the details of the chemical events on the active sites of catalysts where it is notoriously difficult to obtain a molecular description either experimentally or theoretically because of the large metal atom domains that have to be understood and explained. Their importance in catalysis and other important industrial processes was recognised and stressed at an early stage by the late Muertties[2] and Ozin[3] and others. There have been many symposia and reviews published on the topic.[4]

The pioneering EPR studies on naked metal clusters, by Weltner[5] and Lindsay[6] and co-workers have been cardinal in laying the foundations for most subsequent EPR investigations of these intriguing intermediate states of matter. However, most of the Periodic Table remains unexplored and metal clusters remain a challenge both experimentally and theoretically. In this paper we describe the way that electron paramagnetic resonance (EPR) spectroscopy in conjunction with matrix-isolation techniques has responded to that challenge.

Experimental

Principle of the rotating cryostat technique

In the matrix-isolation technique reactive species are trapped and tethered in specific sites in the matrix so that they cannot diffuse to collide with each other and react.[7] The rotating-cryostat variant has been described in detail elsewhere,[8] and here we give only its principal features (Fig. 1).

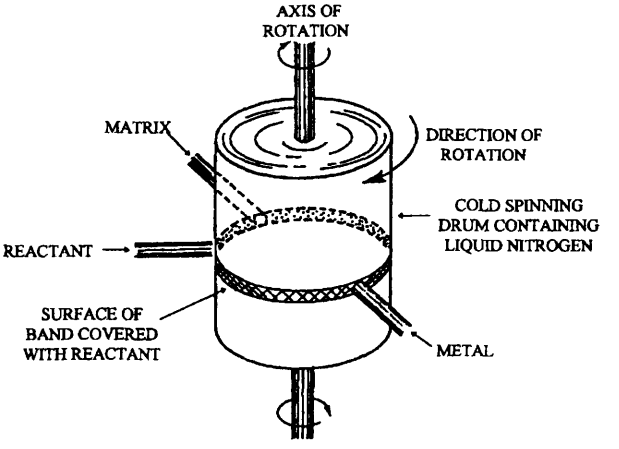

Fig. 1 Principle of the rotating cryostat [reproduced from ref. 8(*c*) with permission]

A drum (12 cm diameter, containing liquid nitrogen) rotates rapidly (> 2000 rpm) in a high vacuum ($< 10^{-6}$ Torr) and the inert matrix (about 10 monolayers per revolution) and metal vapours (< 0.04 monolayer) are rapidly condensed (< 1 ms) in sequence on to its cold surface from ports situated in the outer housing. One hundred thousand interleaving layers are deposited in *ca.* 15 min. The metal vapours emanate from resistively heated tantalum furnaces (Knüdsen cell) situated only a few millimetres away from the drum surface moving at 50 km h^{-1}. In many of the experiments the metal vapour and the deposited

† Basis of the presentation given at Dalton Discussion No. 1, 3rd–5th January 1996, University of Southampton, UK.

Non-SI units employed: Torr ≈ 133 Pa, eV ≈ 1.60×10^{-19} J.

metal atoms beneath the furnace are illuminated with focused light from either a 250 W medium-pressure mercury lamp, alkali-metal resonance lamps or a 200 W deuterium lamp. At the end of the experiment the deposits are transferred, still at 77 K and under high vacuum, to quartz tubes suitable for insertion at 77 or 4 K into EPR/ENDOR cavities. The ENDOR (electron nuclear double resonance) spectra were recorded on a Bruker 300E spectrometer equipped with the Bruker ENDOR attachment. A Bruker Gaussmeter and frequency counter were used for field and frequency measurements. Hyperfine interactions and g values were calculated by exact solutions of the isotropic spin Hamiltonian and are accurate to ± 0.05 mT and ± 0.0001, respectively. A program kindly provided by Dr. K. F. Preston (National Research Council, Canada) was used for this purpose.

The heteronuclear metal clusters were prepared by the simple expedient of vaporising both metals from the same Knüdsen furnace containing a bimetallic alloy of prescribed composition calculated assuming Raoult's law to be applicable.

In those experiments where the reaction between clusters and other molecules were studied the substrate vapour was introduced through a jet interposed between the metal vapour furnace and the matrix jet.

The metals were usually obtained from Goodfellow and were of a purity greater than 99.99%. Most of the organic compounds were obtained from Aldrich and of AnalaR standard and used without further purification in most cases. Adamantane was purified by sublimation.

Four EPR spectrometers have been used, a Varian E-109, a Varian E-9, a JEOL RE 201X and a Bruker 300-E series. All were operated at X band with 100 kHz field modulation and phase-lock detection at this frequency.

Results and Discussion

EPR spectroscopy: advantages and limitations in the study of metal clusters

Before launching into the paper proper, it is worthwhile noting the advantages and limitations of EPR in this area. The important parameters provided uniquely by EPR spectroscopy are: the number of atoms in the cluster, *i.e.* its stoichiometry; the nuclear hyperfine interactions which lead to the unpaired electron spin densities at the different nuclei in the cluster; and the g value which together with the hyperfine interaction values give the contributions of s, p and d orbitals to the SOMO (singly occupied molecular orbital) of the cluster. Often when coupled with quite simple MO considerations the symmetry of the spin distribution and spectra lead inevitably to structural symmetry constraints and an unequivocal determination of the geometry of a cluster.

The most fundamental limitation of EPR is that only paramagnetic species are observable which usually excludes from study most even-numbered clusters. The second practical limitation arises from the fact that EPR spectra of most species are centred in the same region of magnetic field (≈ 330 mT at X-band frequencies of ≈ 9 GHz). The number of transitions from n_i equivalent nuclei with nuclear spin quantum number I_i is multiplicative being $\Pi_i(2n_iI_i + 1)$ in first-order theory and $\Pi_i(2I_i + 1)^{n_i}$ in second-order theory. For example, for seven equivalent copper nuclei the number of possible lines is 22 in first order and 16 384 in second-order theory. The resulting congestion coupled with the diminishing value of the hyperfine interactions as the unpaired electron is 'shared' between increasing numbers of nuclei has put an experimental limit of $n = 13$ on clusters that can be studied at present by EPR, *e.g.* Sc_{13}.[9]

As in many other spectroscopic studies of metal clusters the ideal of monodisperse metal clusters achieved by the soft landing of just one type of metal cluster is still a gleam in the eye of the experimentalist, though some progress has been made in this direction. The often, large values of the hyperfine interactions in the spectra of metal clusters usually necessitate deployment of second- and higher-order perturbation treatments and are one of the interesting aspects of this field to the specialist EPR spectroscopist.[10] Another interesting aspect of metal clusters is their very direct exhibition of the Jahn–Teller theorem[11] and of rovibronic states.[12] Several such effects and examples will be discussed in this paper.

The ENDOR[13] variant of EPR may provide one way of removing some of the problems of congestion and small unresolved hyperfine interactions and hence allow much larger clusters to be studied by magnetic resonance techniques. We provide an encouraging start by reporting here the first ENDOR spectrum of a metal cluster Li_3.

Trimeric clusters

Although it would be logical to start with cluster dimers, the spectra of these species are very complicated and require a sophisticated understanding of EPR theory and are therefore not appropriate for this particular discussion. Hence we start with the trimers. Most of the Periodic Table lies unexplored since only the trimers of Groups 1, 3, 11 and 13 metals have been observed by EPR spectroscopy. Those of the alkali and coinage metals are bonded mainly through the interactions of one s electron in the outer s orbital of each atom and can be readily understood in terms of simple molecular orbital (MO) theory (Fig. 2).

The bonding involves two electrons in a symmetric $1a_1$ orbital in all geometries. In the equilateral triangle configuration there are two degenerate e_g orbitals which the unpaired electron

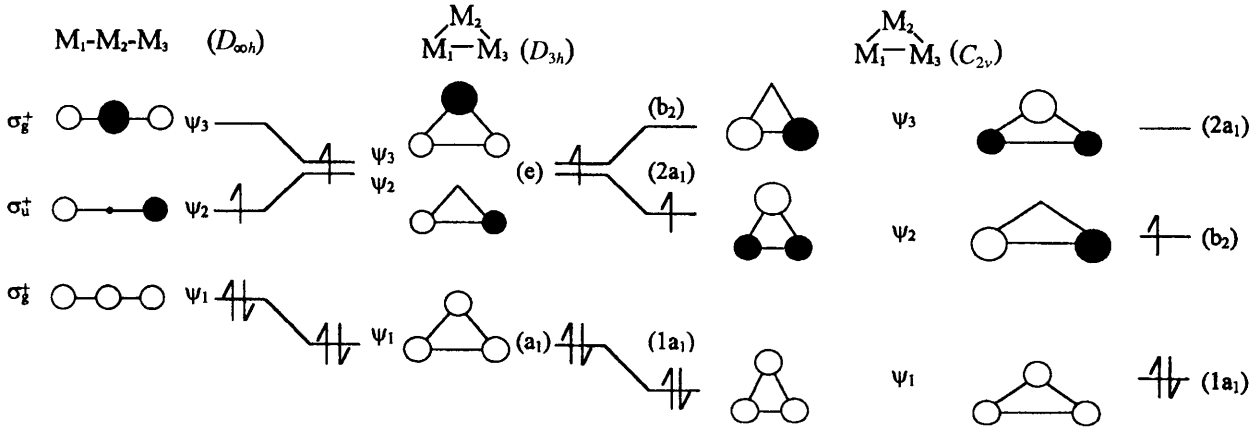

Fig. 2 Molecular orbital correlation diagram linking the structures of linear, equilateral, acute and obtuse triangular trimers, M_3, constructed from atoms with one unpaired s electron

could occupy. The Jahn–Teller theorem [11] requires distortion to produce either an acute or an obtuse/linear structure so that the degeneracy of these two orbitals is lifted (see, however, ref. 10 where it is argued that spin–orbit coupling can remove the requirements of the Jahn–Teller theorem for distortion).

In the acute form the spin density is 0.25 at the two terminal nuclei and 0.5 at the apical nucleus. In both the obtuse and linear structures the spin density is 0.5 at the two terminal nuclei and zero at the apical position. These totally different spin distributions for the two possible distortions can be readily distinguished by EPR spectroscopy and examples of both types of distribution have been observed and are described here.

The alkali-metal group. *Static* Na_3 *and* K_3 *clusters.* We start with Na_3 and K_3 because there are additional subtleties for Li_3 which are discussed later. In rare-gas matrices the EPR spectra of both Na_3 and K_3 consist of septets of quartets giving unequivocal evidence for either an obtuse or linear structure. In this case EPR spectroscopy cannot distinguish between these two possibilities, but it is possible to delineate when g anisotropy is observed (see Ag_3 below).

Fluxional trimers. In addition to the septets of quartets observed for obtuse Na_3 and K_3 in rare-gas matrices there are ten transitions from a carrier showing equal interactions of 261.0 and 68.9 MHz with three equivalent sodium and potassium nuclei respectively.[6,14] This does not indicate an equilateral triangle in contradiction of the Jahn–Teller theorem but is an example of a pseudo-rotating Jahn–Teller molecule, an extreme example of a fluxional molecule with very low energy barriers separating 'isomeric' structures. The potential-energy surface for the trimers resembles a 'Mexican Hat' with the equilateral triangular structure at the high-energy central peak while the three equivalent obtuse structures lie at three equivalent wells M_1, M_2, M_3 along the rim contour (Fig. 3). The three saddle points C_1, C_2 and C_3 separating the three minima are at the conical intersections of their potential-energy curves. In an adamantane matrix only the fluxional Na_3 trimer with all 10 lines present was observed even at 4 K, indicating barriers of $\leqslant 1$ kJ mol^{-1}.[15] In argon the rate of pseudo-rotation never quite ensures complete averaging so that only four transitions are observed[14] (those with $M_I = \pm\frac{7}{2}, \pm\frac{5}{2}, \pm\frac{3}{2}$ being broadened beyond detection). This, together with the occurrence of a static form in argon and a significant dynamic frequency shift, argue for greater matrix perturbation of the cluster in rare-gas matrices than in adamantane.

The Li_3 trimer is an extreme example of a rovibronic molecule because it is seen only in the fluxional form even at 4 K in both inert-gas and hydrocarbon matrices.[16,17] The absence of spectral lines from the obtuse form of Li_3 even in inert-gas matrices at 4 K presumably arises because of the smaller size of the cluster. Yet again this indicates that the static forms of the alkali-metal trimers in the inert-gas matrices persist mainly because of matrix perturbations. The extreme case of matrix perturbation is of course chemical bonding between the trapped species and matrix molecules. For example, we have found such bonding in Na_3 when traces of water are present (see below).

These alkali-metal fluxional trimers are examples of rovibronic coupling in molecules where the usual Born–Oppenheimer approximation no longer applies because the electronic and nuclear motions are coupled together and are not separable.[12] There have been numerous theoretical calculations of the behaviour of the alkali-metal trimers and many estimates made of the Jahn–Teller energy barrier for motion between the shallow potential wells.[18] These estimates place the barrier at less than 1.5 kJ mol^{-1} for all the alkali-metal trimers, including Na_3 and K_3. The ENDOR spectrum of Li_3 provides complete confirmation that all of the atoms are equivalent in this cluster at 20 K in an adamantane matrix (see below).

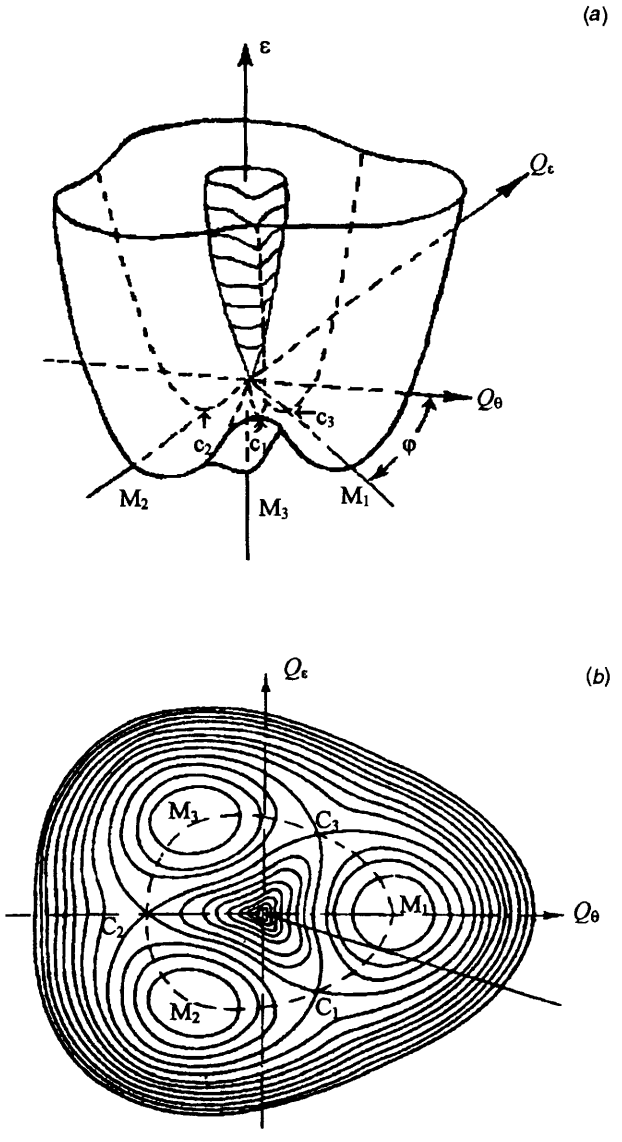

Fig. 3 (*a*) Mexican Hat potential-energy contour surface for a trimeric molecule exhibiting vibronic–electronic coupling (ε is the potential energy, Q_ε, Q_θ and ψ are the symmetrised normal coordinates of the molecular vibrations). (*b*) The contour diagram for (*a*). The potential minima are the $^2B_2$ states, while the cols are the $^2A_1$ states and the central high maximum is the Jahn–Teller-forbidden D_{3h} state. (Reproduced from ref. 12 with permission)

Acute Na_3 *cluster.* The acute Na_3 cluster is not a naked cluster but one associated with water molecules. It is only observed when traces of water are introduced into an adamantane matrix ($< 10^{-2}$ monolayer of water interleaving 10 monolayers of adamantane per revolution of the cryostat drum). Fig. 4 shows the EPR spectrum at 77 K of sodium vapours deposited into this water-doped adamantane matrix. Despite the complexity of the spectrum, because it is a composite of transitions from many species, it can be analysed by comparing it with the spectra from sodium vapour deposited in the absence of water. The spectral assignments are given in Fig. 4. Transitions c and x are only observed when water vapour is present. The c features can be assigned to a sodium atom–water complex, $Na(H_2O)$, similar to the $Li(H_2O)$ complex which has been previously observed in inert-gas matrices by Margrave's group[19] and by us.[15] The remaining transitions, x, whose prominent features are most clearly observed away from the congested central regions of the spectrum, are assigned to an acute cluster associated with water, $Na_3(H_2O)_x$, $x \geqslant 1$.

The quartet of septets, x, which are clearly resolved from

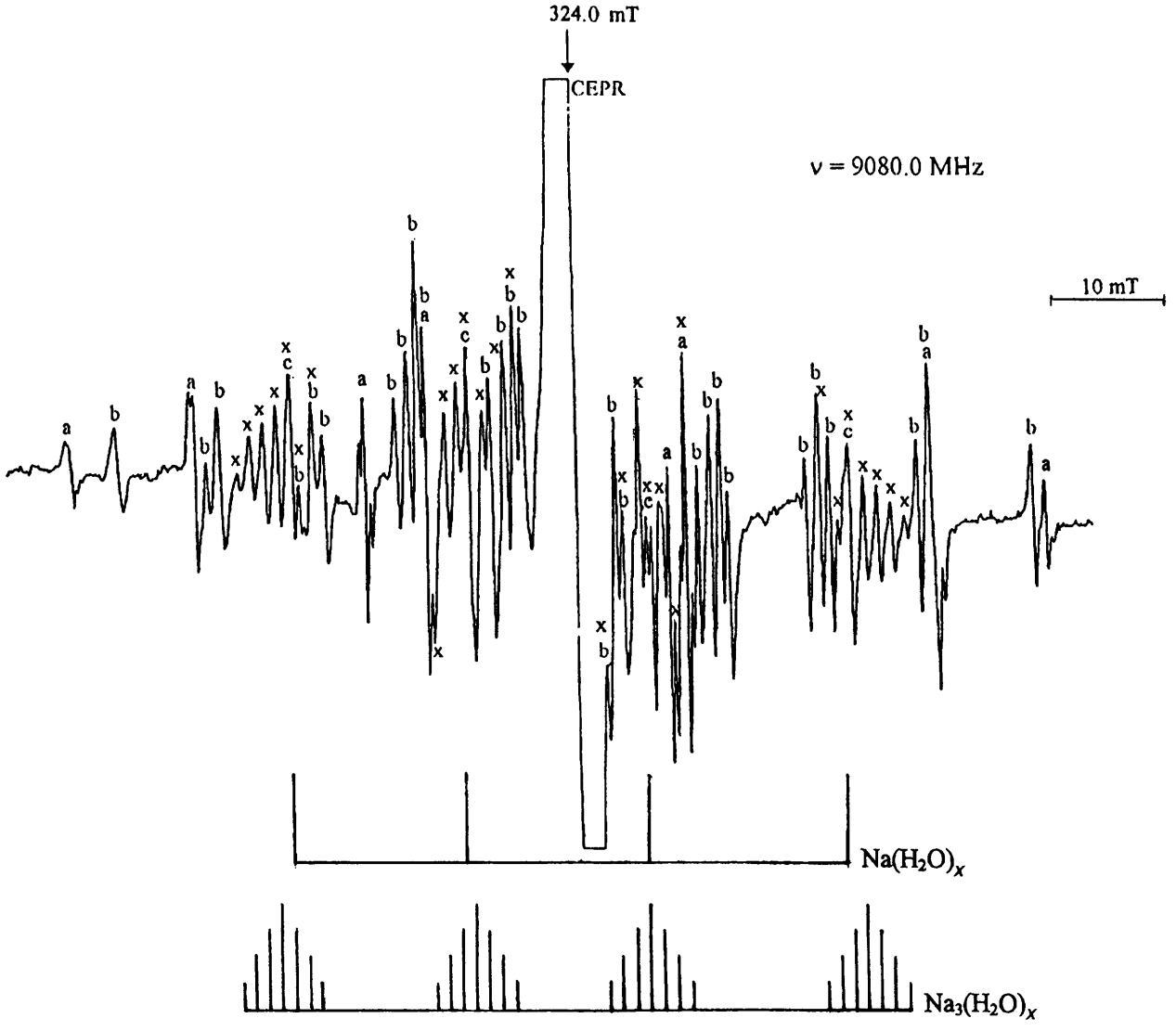

Fig. 4 The EPR spectrum at 77 K of the acute form of Na_3 in an adamantane matrix containing traces (< 0.01 monolayer) of water. Spectral assignments are: a, Na atoms; b, Na_3 (fluxional); c, $Na(H_2O)$; x, $Na_3(H_2O)_x$ acute. CEPR = Conduction EPR

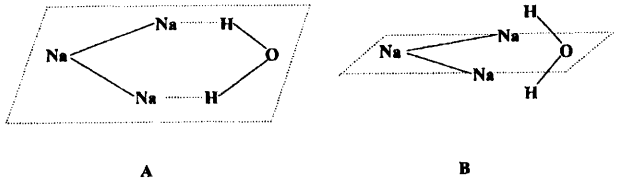

A B

other transitions are readily assigned to a doublet carrier which has a large isotropic hyperfine interaction of 503.3 MHz with one sodium nucleus and a much smaller interaction with two other equivalent nuclei. An exact solution of the spin Hamiltonian gives the following EPR parameters for this species: $g = 2.001$; $a_{Na}(1) = 503.3$ MHz and $a_{Na}(2) = 35.0$ MHz.

As already discussed such a distribution is consistent with only an acute-angle molecule with a $^2A_1$ ground state in C_{2v} symmetry. Division of the observed hyperfine interactions by the one-electron parameter for unit spin density in a sodium 3s orbital (885.8 MHz) gives spin densities of 0.57 on the apical nucleus and 0.04 on the two terminal nuclei. Both simple and sophisticated MO calculations indicate that the signs of the spin will be the same on all nuclei in a $^2A_1$ ground state. If all the spin densities are positive then a total s-spin density of 0.65 results. There is a reduction of 22% in the total spin density compared with that in the uncomplexed obtuse and the fluxional Na_3. This indicates either a 22% delocalisation of the unpaired electron on to the associated conjugate water molecule(s) or a similar percentage increase in the p-orbital contribution to the SOMO in $Na_3(H_2O)_x$.

We suggest two possible structures **A** and **B** for a monowater complex, $Na_3(H_2O)$, but cannot exclude a structure with an oxygen of the water molecule next to the cluster or other structures where more than one molecule is interacting. Unfortunately no proton hyperfine interaction is observed in the EPR spectrum but preliminary ENDOR studies indicate that they are of the order of 0.8 MHz.

The change in structure of a small cluster, such as Na_3, on the approach of a reactive molecule, such as water, is important in two respects. First it is a direct demonstration of the dynamic nature of clusters and has important implications in the modelling of the active sites in heterogeneous catalysis. Clearly, the active site is not simply a template but a dynamic flexible structure which can change shape as the substrate molecule approaches and can then return to its original shape as a product molecule departs, *cf.* the opening and closing of a fist clenching a ball of clay. Such flexibility may be reduced by attachment of the cluster to supports but the clusters themselves are intrinsically flexible. Secondly, it shows the extent to which

matrix perturbations can favour one of two closely similar ground states.

A heteronuclear cluster Na_2Li. No one has yet reported the EPR spectra of matrix-isolated heteronuclear alkali-metal clusters formed by codepositing two metal vapours from two separate furnaces either on to static or moving cold matrices. However, the detailed and comprehensive theoretical calculations of Gole and co-workers[20] predict that such mixed clusters should have high binding energies of *ca.* 120 (NaLiNa) and 96 kJ mol^{-1} (LiNaNa). Because of the subtle differences between the trimers of the alkali metals we were interested in preparing and examining mixed trimers of Li and Na/K.

We have succeeded in generating the mixed cluster NaLiNa by covaporising mixtures of sodium and lithium (*i.e.* alloys) from the same Knüdsen furnace. Similar methods have been deployed by Morse[21] and Weltner[22,23] and co-workers for preparing dimeric clusters. Ratios Na:Li of 1:4 to 1:6 and Knüdsen cell temperatures of 890–930 K were used to produce vapours containing equal proportions of both elements. We have as yet not been able to assign unequivocally transitions from other possible Na/Li and Na/K mixed trimers although the septamer Na_2K_5 has been prepared and is described later.

Fig. 5 shows the EPR spectrum at 77 K from the codeposition on to 10 monolayers of adamantane of 4×10^{-3} Torr each of sodium and lithium from the same furnace. All the transitions, except those labelled x and y, have been previously assigned and arise from isolated atoms and homonuclear clusters.[24] The y transitions are presently being analysed and may well be from other mixed Na_xLi_y clusters. The x transitions can be assigned unambiguously to a mixed static obtuse-angled trimer NaLiNa because of the following observations. The quartet of lines, spaced by 9.8 MHz, which were resolved on annealing the sample to 170 K (shown in the inset of Fig. 5) clearly demonstrate the presence of only *one* Li atom in the cluster. These multiplets are associated with transitions arising from a larger hyperfine interaction of 354.8 MHz with *two* equivalent sodium nuclei showing that the stoichiometry of the carrier is Na_2Li. Because of the size of $a^2/4H$ (a is the hyperfine interaction and H the magnetic field) there is a complete separation of all the second-order $(2I + 1)^n$ transitions so that sixteen lines result, not the seven $(2nI + 1)$ lines expected from a first-order treatment for $I = \frac{3}{2}$ and $n = 2$. The spin densities calculated from these EPR parameters are 0.40 at each Na and 0.02 at the Li. If the latter is negative, since it is likely to arise by bond polarisation, we estimate a total s-spin density of 0.78 which lies between the values of 0.90[15] and 0.69[17] for Na_3 and Li_3 respectively.

In contrast to the other alkali-metal trimers in adamantane, the mixed trimer NaLiNa has a static obtuse-angled geometry, similar to that of the homonuclear trimer clusters of the coinage metals (see later). The potential-energy contour for the homonuclear trimers with low, identical, pseudo-rotational barriers between three equivalent obtuse structures has been replaced by one with two isometric shallow wells with one

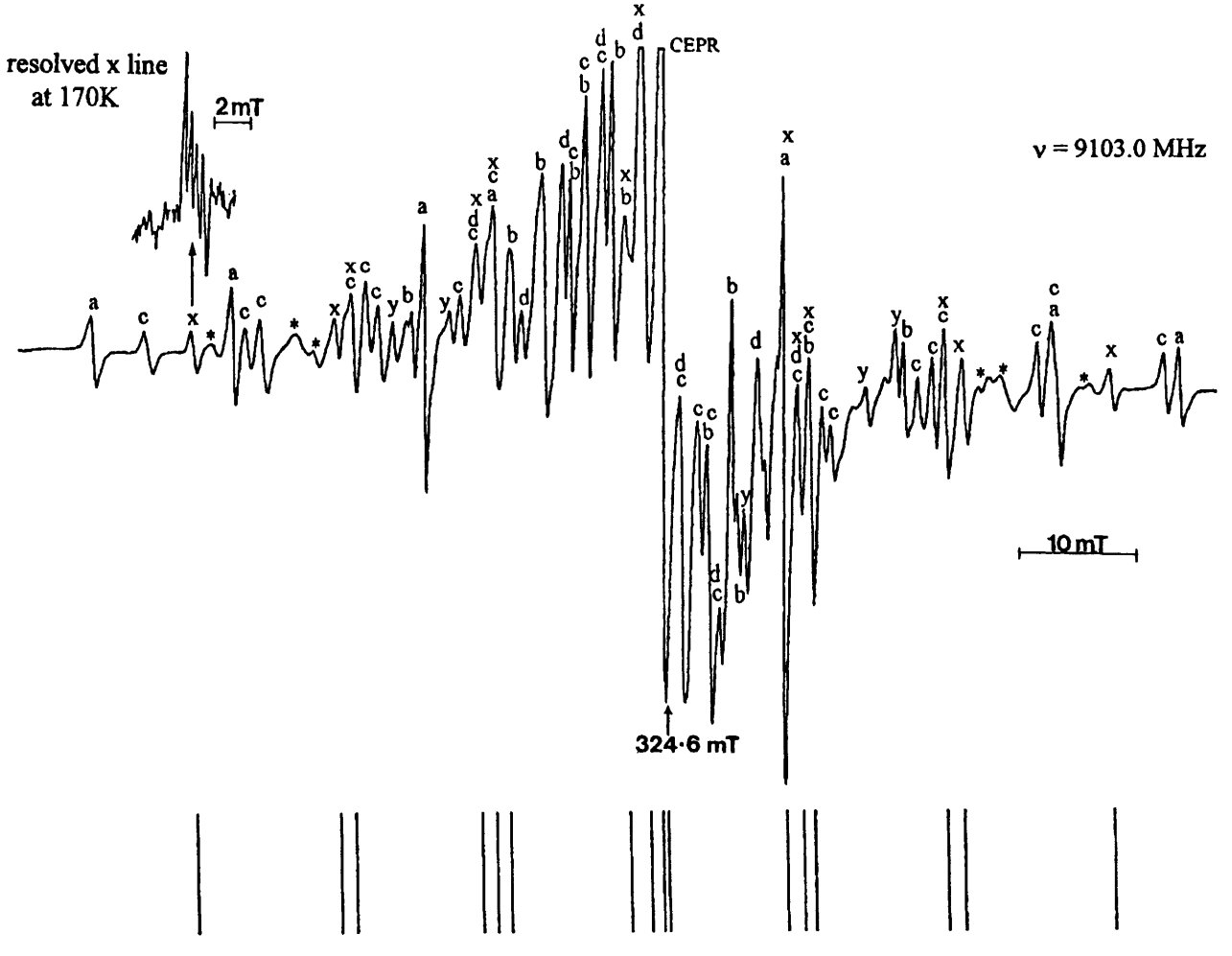

Fig. 5 The EPR spectrum at 77 K of the sample produced from the vaporisation of a Na–Li alloy into an adamantane matrix. The transitions are assigned as follows: a, Na atoms; b, Li atoms; c, fluxional Na_3; d, fluxional Li_3; x, Na_2Li; y, unassigned Na/Li cluster; *, unassigned transitions arising from a sodium species. Transitions x and y are not observed when sodium and lithium are deposited alone at similar concentrations. The stick diagram indicates the predicted line positions based upon the EPR parameters given in the text. The inset shows on an expanded scale the $M_I = +3$ transition of the Na_2Li cluster after annealing to 170 K

sodium at the apical position and one much deeper well with lithium at this unique position. This accords with theoretical diatomics in molecules (DIM) calculations[20] which predict that a lithium-centred obtuse triangle with an apical bond angle of 100° is the most stable structure for Na_2Li. Its calculated binding energy is 120 kJ mol^{-1} compared to 96 kJ mol^{-1} for LiNaNa. However, the most stable trimer is predicted to be LiNaLi (binding energy 137 kJ mol^{-1}) and it is possible that this trimer is the carrier of transitions y in Fig. 5. Theoretical calculations of the spin-density distributions in these mixed trimeric clusters are clearly needed.

The first ENDOR spectrum of a metal cluster Li_3. In order to extend the applications of ENDOR to matrix-isolated species we have attempted to obtain the ENDOR spectrum of the fluxional Li_3 cluster in an adamantane matrix. We present here our preliminary findings. Müssig *et al.*[25] have previously presented the ENDOR spectrum of the dimeric cation Ag^0–Ag^+.

The static magnetic field was locked at the $M_I = +\frac{1}{2}$ EPR transition [marked* in Fig. 6(*a*)] of the fluxional Li_3 cluster, which was then saturated with 100 mW microwave power, while its intensity was monitored as the sample was scanned from 2 to 62 MHz by radiofrequency radiation at 200 W. The resulting ENDOR signal is displayed in Fig. 6(*b*) and shows a major doublet of 11.10 MHz centred at 46.15 MHz. It is a textbook example of a species where $A/2 > \nu_n$ so that the ENDOR lines are centred at $A/2$ and separated by $2\nu_n$, where ν_n is the ^7Li NMR frequency at the magnetic field of the EPR line being saturated. The value of $A = 92.3$ MHz corresponds closely with that of 92.7 MHz previously obtained from the EPR spectrum of $^7Li_3$,[17] but is more accurate. The value $\nu_{Li} = 5.55$ MHz is exactly correct for ^7Li. Thus the major features in the ENDOR spectrum are without doubt those of the $^7Li_3$ fluxional cluster. The two transitions B arise from a ^6Li nucleus in the same cluster [the natural abundance of ^6Li ($I = 1$) is 7.5%]. The separation of the B doublet is exactly that expected from the NMR frequency of ^6Li ($2\nu_{Li}$) at a field of 335.5 mT. However, the centre of the doublet gives a somewhat larger A value of 37.1 MHz than that calculated from the ^7Li hyperfine interaction and the ratio of ^7Li:^6Li hyperfine interactions (34.2 MHz). Lindsay found exactly the calculated A value for $^6Li_3$. We speculate that the larger than expected A value for ^6Li in $^7Li_2{}^6Li_6$ may result from the fact that the two structures with the lighter ^6Li isotope located at the terminal position, $^6Li^7Li^7Li$, may have slightly lower energy than that with the ^6Li at the central position $^7Li^6Li^7Li$. This could result in an unequal averaging and hence a larger ^6Li coupling. The effects of temperature on the position of the B doublet could possibly be used to estimate the differences in depths of the wells. Moskovits *et al.*[26] in their original report of Cu_3 discussed such isotope effects though the detailed analysis has now been modified.[27] The other weaker transitions in Fig. 6(*b*) are thought to be due to Li_3 clusters associated with water molecules and will be discussed in a subsequent paper. The ENDOR spectrum of Li_3 confirms that all the lithium nuclei are equivalent on the EPR/ENDOR time-scales since two sets of ENDOR doublets from two different nuclei would have been observed from either acute- or obtuse-triangled structures.

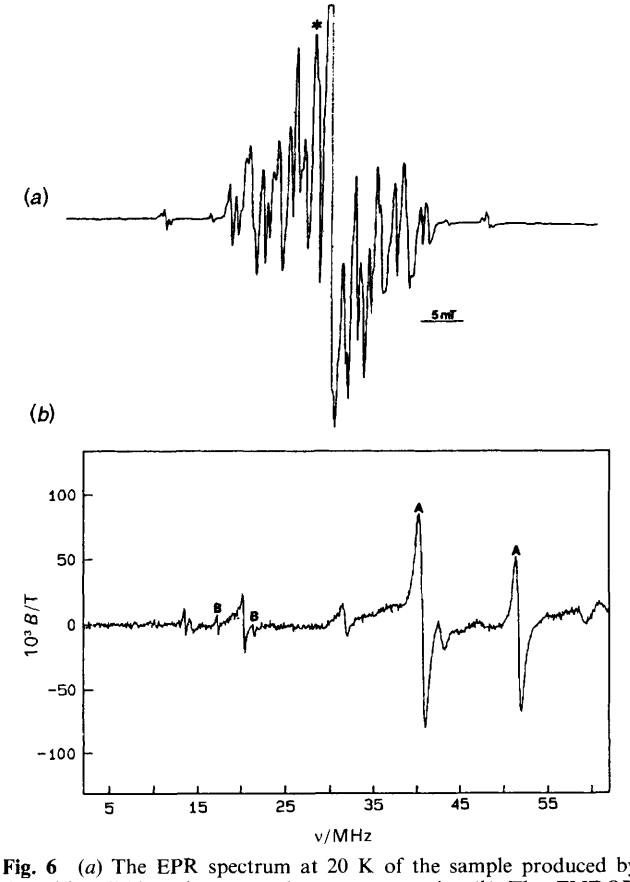

Fig. 6 (*a*) The EPR spectrum at 20 K of the sample produced by depositing lithium into an adamantane matrix. (*b*) The ENDOR spectrum in which the $M_I = +\frac{1}{2}$ transition of Li_3 has been saturated with 100 mW microwave power and the sample exposed to 200 W of radiofrequency power

We are encouraged by this first recording of the ENDOR spectrum of a cluster and are now extending our ENDOR studies to the other alkali-metal and coinage-metal clusters. We are hoping to use general triple resonance to obtain the, as yet, undetermined signs of the spin densities at the different nuclei in these and other clusters. The results will provide a severe test of the validity of current sophisticated MO calculations of such clusters.

Trends and puzzles. In Table 1 we list all the known EPR parameters for alkali-metal trimers while Fig. 7 shows the energy levels of the isolated alkali and coinage metal atoms.

The observation of both static and fluxional forms of Na_3 and K_3 in inert-gas matrices immediately allows us to determine that the spin density at the apical position is negative. In this case the total spin densities are 0.87 and 0.89 for static Na_3 and K_3, respectively. If the spin density on all the nuclei were of the same sign the values would be 1.00 and 1.04. The 'experimental' average $\Sigma\rho_i$ values from the fluxional molecule are 0.87 and 0.90; thus the spin density is negative at the unique position.

There is a monotonic increase in the total s-spin density in the homonuclear congeners as the Periodic Table is ascended with no reversals as will be seen to occur for the coinage metals (see later). There are corresponding decreases in the bond strengths (kJ mol^{-1}) in the alkali-metal dimers: D(Li–Li) = 201, D(Na–Na) = 71.1, D(K–K) = 55.6, D(Rb–Rb) = 45.2 and D(Cs–Cs) = 38.[28] It is not too apparent why there is more

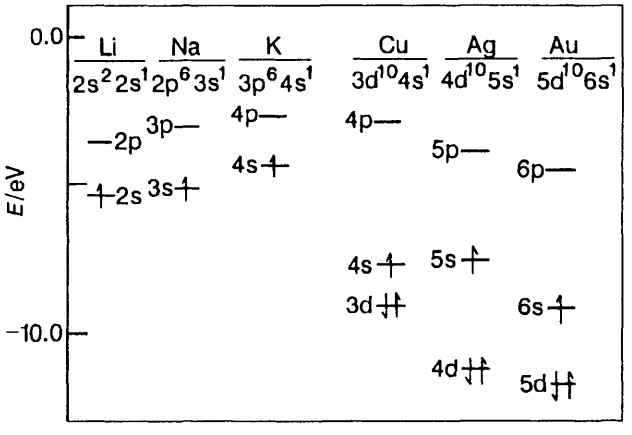

Fig. 7 The energy levels of the alkali and coinage metals

Table 1 The EPR parameters of Group 1 metal trimers

Cluster	Matrix	a_m [a]	a_o [b]	a_3 [c]	$\Sigma\rho_i$ [d]	g
$^7Li_3$	$C_{10}H_{16}$	92.7	—	—	0.69	2.001
$^7Li_3$	Ar	90.2	—	—	0.68	2.0026
Na_3	$C_{10}H_{16}$	262.2	—	—	0.87	2.0016
Na_3	Ar	261.0	—	—	0.87	2.0012
Na_3	Ar	—	418.7	63.3	0.87	2.0012
Na_3 (acute)	$C_{10}H_{16}$ (H_2O)		35.0	503.3	0.65	2.001
K_3	Ar	68.9	—	—	0.90	1.9990
K_3	Ar	—	109.2	13.2	0.89	1.9985
Na_2Li	$C_{10}H_{16}$		354.8	9.8	0.78	2.001

^{7}Li atoms gas phase, a_o = 401.7; ^{23}Na atoms gas phase, a_o = 885.8; ^{39}K atoms gas phase, a_o = 2308.8. Units of hyperfine interaction are MHz. [a] Fluxional cluster. [b] Terminal hyperfine interaction. [c] Central hyperfine interaction in static cluster. [d] $\Sigma\rho_i$ is the total spin density.

2p orbital contribution in Li_3 than 4p contribution in K_3 since the energy gap is virtually the same. The reason for the existence of both static and fluxional forms of Na_3 and K_3 while Li_3 exists only as a fluxional molecule despite its stronger bonding is not clear. It appears likely that the non-fluxional forms of Na_3 and K_3 observed in an argon matrix may result from the larger size of these clusters which are thus prone to larger perturbations in the smaller substitutional sites of these matrices. The absence of such static forms in adamantane indicates that such perturbations are less important in its larger substitutional sites.

No matrix-isolated clusters of caesium or rubidium have ever been observed which is perhaps not surprising considering the very weak bonds even in their dimers.

The coinage metals. Unlike the alkali-metal trimers only the static ground states of the three coinage metals copper, silver and gold have been observed by EPR spectroscopy.[29-31] There have been no reports of matrix-isolated fluxional coinage-metal clusters showing that their pseudo-rotational barriers in matrices are large enough to maintain the static configuration for times greater than (hyperfine interaction) $^{-1}$. The results of gas-phase studies on molecular beams of Cu_3 by resonant two photon ionisation and other techniques also cannot be fitted to a simple potential model with a completely fluxional ground-state trimer, thus confirming the matrix-isolation results. However, the barriers estimated from these gas-phase studies are exceptionally small, < 2.6 kJ mol^{-1}.[32]

If correct, these small barriers for 'free' gas-phase clusters imply that for matrix-isolated clusters the matrix perturbations must be larger than ≈ 10 kJ mol^{-1} to stop the fluxionality at 77 K and higher. The limit of such perturbations is of course the formation of a definite complex between the trimer and a matrix molecule and indeed an example of such a complexation has already been discussed for $Na_3(H_2O)_x$ and $Ag_3(C_2H_4)_y$ and possibly $Ag_3(N_2)_x$ and $Cu_3(N_2)_x$.[31] The EPR spectra and parameters of the homonuclear coinage trimers have been thoroughly discussed and summarised elsewhere.[29-31,33] Here we report on a new heteronuclear trimeric cluster Au_2Ag produced by the covaporisation of gold and silver alloys.

A new heteronuclear trimer, Au_2Ag. There has been only one report of a mixed coinage-metal trimer, Cu_2Ag, prepared by depositing copper vapour and silver vapour from separate furnaces on to a rotating cryostat drum using a benzene matrix.[34] It has an obtuse geometry with a $^2B_2$ ground state in C_{2v} symmetry.

In order to prepare the mixed gold–silver trimer furnace temperatures from 1900 to 2000 K are required. Natural silver with both ^{107}Ag and ^{109}Ag isotopes was used together with a deuteriated benzene matrix. The yields of the gold-containing cluster were enhanced by illumination with light from a 200 W deuterium lamp which provides sufficient energy to excite the gold 6p ← 6s transition.

Fig. 8 shows the EPR spectrum at 77 K of a sample of vaporised Au/Ag in deuteriated benzene. It is dominated by the transitions of gold and silver mono- and di-benzene complexes[8b] and a multiplet of lines in the central region due to homonuclear Ag_3 trimers.[33] However, in addition to these major transitions there are a number of weaker isotropic doublets which are most clearly seen away from the central congested region of the spectrum and are indicated in the insets of Fig. 8. These doublets were only observed when silver was covaporised with gold (the anisotropic features Y are also only observed when gold and silver are covaporised but have not yet been fully assigned). The doublets of the gold–silver cluster indicate a carrier in which there is a small hyperfine interaction with one silver nucleus. There is a large hyperfine interaction with two gold nuclei but only four of the expected 16 doublets are well resolved because of the spectral overlaps in the central region of the spectrum. An exact solution of the spin Hamiltonian gives the following EPR parameters: g = 1.9292; $a_{Au}(2)$ = 1182.6 MHz, $a_{Ag}(1)$ = 36.4 MHz. These lead to spin densities of 0.39 and 0.02 at the terminal Au atoms and central Ag atoms, respectively, and give a total spin density of $\Sigma\rho_i$ = 0.76. These parameters indicate that the Au_2Ag cluster has two terminal gold atoms and one apical silver atom in an obtuse-angle structure with a $^2B_2$ ground state in C_{2v} symmetry.

Trends. There are several features of the coinage-metal trimers which require comment. The first is the lack of observation of the EPR spectra of any of these clusters in inert-gas matrices at much lower temperatures. There is no obvious reason why these clusters are not observed, especially when the alkali-metal clusters are so readily made and show clear and sharp EPR spectra. The second puzzling feature is the different structures of Cu_3 and Ag_3 that exist in solid nitrogen and hydrocarbon matrices. They are obtuse in the latter and acute in the former.[29-31,33]

Numerous theoretical calculations on these coinage-metal clusters show that the energy differences between the ground states of these two geometries[35] are small, < 1.2–2.4 kJ mol^{-1}. Lindsay and co-workers[29] have suggested that the matrix perturbations could easily be of this order of magnitude. While that may well be the case, it is also possible that the nitrogen in the solid nitrogen matrix acts not as a perturbator but as a chemical entity forming weak bonds with the Cu_3 and Ag_3 clusters and hence encouraging the adoption of an acute-angled structure. This is made more feasible by our observations of the change in structure of an Na_3 cluster when interacting with water molecules. The fact that the total spin densities are virtually identical for both acute and obtuse configurations of the trimers argues against appreciable spin delocalisation on to adjacent nitrogen molecules in the solid nitrogen matrix.

The spin densities in the trimers as the periodic group is ascended from copper to gold (Table 2) show an interesting reversal. In going from Cu_3 to Ag_3 there is an increase at the

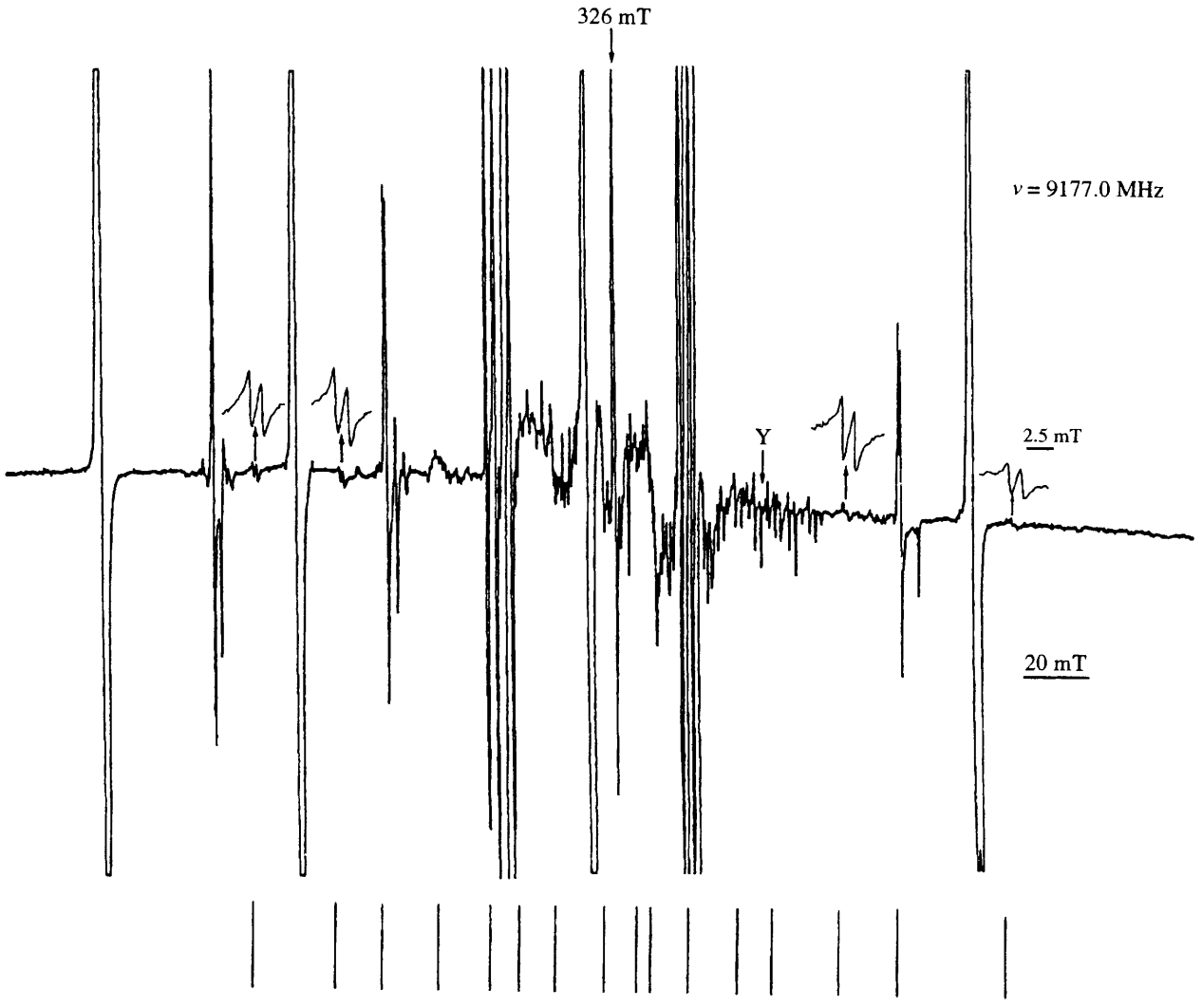

Fig. 8 The EPR spectrum at 77 K of Au and Ag covaporised into a perdeuteriobenzene matrix. The transitions due to Au_2Ag are shown at a higher gain as insets on the main spectral line. The other major transitions are from $Au(C_6D_6)$, $Au(C_6D_6)_2$, $Ag(C_6D_6)$ and $Ag(C_6D_6)_2$ complexes

Table 2 s-Spin populations in trimers of Group 11 metals

Trimer	Matrix	ρ_0 (2)	ρ_3 (1)	$\Sigma_i\rho_i$
Cu_3	$C_{10}H_{16}$	0.29	−0.026	0.55
	N_2	0.13	0.36	0.62
Ag_3	C_6D_6	0.44	−0.06	0.82
	N_2	0.12	0.51	0.75
Au_3	C_6D_6	0.39	−0.056	0.72
Cu_2Ag	C_6D_6	0.41	−0.04	0.78
Au_2Ag	C_6D_6	0.39	−0.02	0.76

ρ_0 is the spin population on the two terminal atoms and ρ_3 that on the central atom.

terminal atom and in the total spin density $\Sigma\rho_i$ but on further ascending to Au_3 there is a reduction in both.

The change from Cu_3 to Ag_3 is due mainly to the much closer spacing of the copper 3d and 4s levels (1.4 eV) compared to the silver 4d and 5s spacing of 3.7 eV. The increase in s-spin density in Au_3 is partly explained by the lower value of 2.6 eV for its 5d to 6s spacing but may also be an interesting illustration of relativistic effects in the chemistry of heavy metals. Similar reversals in going from silver to gold are seen in other parameters such as the bond lengths and vibrational frequencies of di- and tri-meric gold and silver clusters. We base our argument on that given by Bishea and Morse[36] in their lucid account of these reversals of the properties of the coinage metals. As the electron penetrates near the gold nucleus with its high positive charge of 79+ its speed approaches that of light with a resultant relativistic increase in its mass. This in turn leads to a relativistic contraction of those orbitals with high electron densities at the nucleus (s orbitals), while the less-penetrating orbitals (p, d and f) are better shielded by these contracted s orbitals and therefore expand relatively. This expansion increases the contribution of these latter orbitals to chemical bonding and *vice versa* the contribution of the s orbitals is lowered because of their contraction. Thus the s-orbital spin density in Au_3 will also be lower than in Ag_3 for this rather subtle reason.

Septamers of the alkali and coinage metals

The EPR spectra of the septamers of the coinage metals and the alkali metals have been extensively studied by three groups: Weltner's in Florida;[37,38] Lindsay's[39,40] in New York and ours in Ottawa and Britain.[31] The spectra of all the septamers show a large hyperfine interaction with two nuclei and a much smaller hyperfine interaction with the remaining five nuclei. The EPR spectrum of Cu_7 in a C_6D_{12} matrix is shown for illustration in Fig. 9. (This spectrum illustrates the problems of determining the stoichiometry of clusters above $n = 5$ and indeed was originally assigned incorrectly to Cu_5 rather than Cu_7.) These observations are entirely consistent with the pentagonal-bipyramidal geometry for the cluster which is predicted theoretically.[41–45] The pentagonal symmetry of this reasonably large cluster is of some interest because of the importance of this symmetry in the nucleation and growth of small clusters

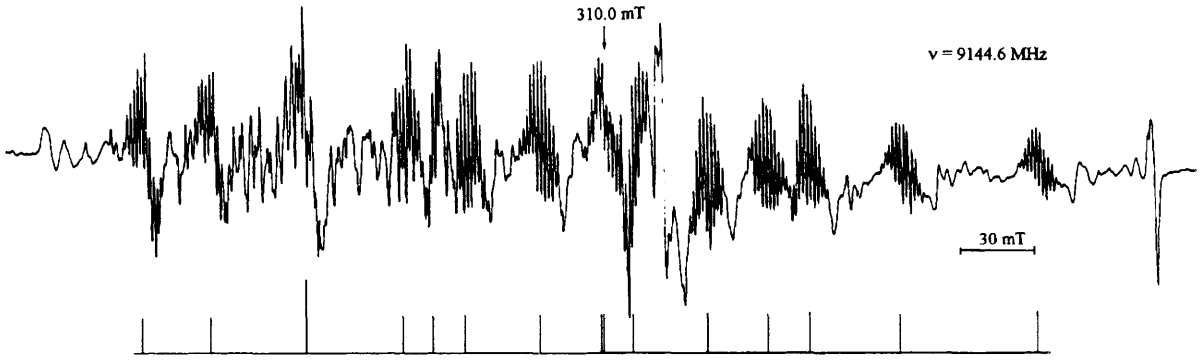

Fig. 9 The EPR spectrum of Cu_7 in a C_6D_{12} matrix at 77 K

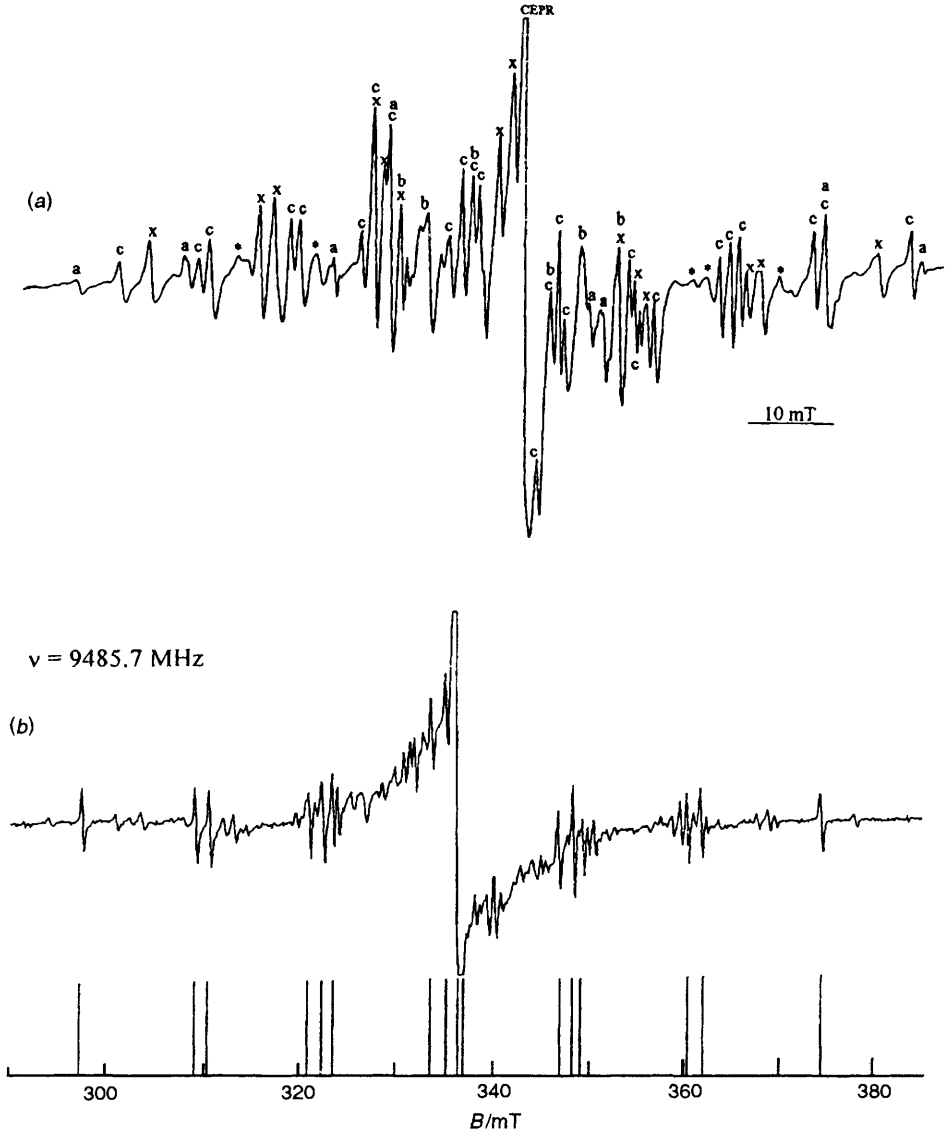

Fig. 10 (*a*) The EPR (77 K) spectrum of the sample produced by depositing a Na–K alloy on to a rotating cryostat drum. Transitions: a, Na atom; b, K atom; c, Na_3 (fluxional); x, Na_2K_5; *, as yet unassigned, arising from a sodium-only species. (*b*) The EPR spectrum of Na_2K_5 at 180 K. The stick diagram indicates the predicted line positions based on the EPR parameters given in the text

and nanoparticles.[46] Even simple molecular orbital calculations predict an electron configuration $(a_1'')^2$, $(e_1')^4$ $(a_2'')^1$ in a $^2A_2''$ ground state. We report here the new EPR spectrum of a septameric heteronuclear cluster, Na_2K_5.

The cluster was again prepared by co-evaporation of a sodium–potassium alloy from the same Knüdsen furnace into an adamantane matrix.[47] Fig. 10(*a*) shows the EPR spectrum from the deposit at 77 K. Again, although composite and therefore complex, the complete spectrum containing five species in all can be satisfactorily analysed and most of the transitions assigned to established species and to the new sodium–potassium cluster. The spectral assignments are given in the legend. The new transitions, x, are most readily seen away from the congested centre of the spectrum. These transitions are only seen when both potassium and sodium are covaporised and do not arise when either metal is vaporised singly from separate furnaces. Power-saturation experiments also showed these transitions to arise from a cluster since they are much

Table 3 Spin populations in septamers of Groups 1 and 11 metals

Septamer	Matrix	ρ_a (2)	ρ_e (5)	$\Sigma_i\rho_i$
Li_7	Ar	0.254	−0.015	0.43
Na_7	Ar	0.374	−0.021	0.65
	N_2	0.350	−0.022	0.59
K_7	Ar	0.371	−0.022	0.63
Na_2K_5	$C_{10}H_{16}$	0.41 (Na)	−0.004 (K)	0.80
Cu_7	Ne	0.291	−0.009	0.54
	C_6D_{12}	0.30	−0.01	0.55
Ag_7	Ne	0.325	−0.012	0.59
	C_6D_{12}	0.30	−0.01	0.55
Cu_2Ag_5	C_6H_{12}	0.30	-	—
$CuAg_5$	C_6H_{12}	0.26 (Cu)	—	—
		0.35 (Ag)		
	Bulk Li	—	—	0.42*
	Bulk Na	—	—	0.66
	Bulk K	—	—	0.66
	Bulk Cu	—	—	0.49
	Bulk Ag	—	-	0.60
	Bulk Au	—	—	0.71

ρ_a and ρ_e are the s-spin populations on the apical and equatorial atoms, respectively; $\Sigma\rho_i$ calculated assuming ρ_e to be negative. * At the Fermi surface of the bulk metal, see ref. 16 for details of these calculations.

less reduced at high power than the readily saturated atom transitions. Careful annealing of the sample to 180 K led to complete disappearance of the atom absorptions and considerable decay of the Na_3 cluster, leaving behind the conduction EPR (CEPR) band and transitions from the mixed cluster [Fig. 10(*b*)].

The isotopic features, x, are due to a double species ($S = \frac{1}{2}$) with a large hyperfine interaction with two equivalent sodium nuclei ($I = \frac{3}{2}$). Again, the hyperfine interactions are so large that there is a complete separation of the 16 lines. The following EPR parameters are derived: $g_{iso} = 1.996$ and $a_{Na}(2) = 362.1$ MHz. It is more difficult to decide on the number of potassium nuclei splitting each main transition into poorly resolved multiplets of 0.98 MHz. Careful simulation of an expanded spectrum of each transition shows that the number of potassium nuclei interacting with the electron is five *i.e.* the spectrum is due to Na_2K_5.

The usual calculations give spin densities of 0.41 at each of the two sodium nuclei and ±0.004 at each of the five potassium nuclei. The very small 4s spin density of potassium could arise from spin polarisation and, therefore, could well be negative. Spin populations of all known septamer clusters are listed in Table 3. There is little doubt that the Na_2K_5 cluster has a $^2A_2''$ ground state with the same electronic configuration as that for the homonuclear Na_7 and K_7 clusters. The departure of the total s-orbital spin density $\Sigma\rho_i$ from unity in this case also implies p and/or d contributions in the SOMO. There is an aspect here which is worth highlighting. If the spin densities at the potassium nuclei are negative then the total spin density is 0.80 but if the spin density at these nuclei is positive then the total spin density in Na_2K_5 is 0.84, a value very close to that in the trimers. This aspect is important because the much lower value of 0.65 for the homonuclear septamers calculated by assuming a negative spin density at the pentagonal nuclei implies p–d orbital contributions of 0.35 which as Lindsay[29] and we[31] have already pointed out is close to the p–d overlap at the Fermi surface of the bulk metal, whereas the higher value of 0.85 implies much greater departure from bulk metal characteristics and indicates a much more molecular structure for the septamer cluster. This is important in the context of answering the question 'how many atoms maketh a metal?'[48] We are attempting to obtain the general triple ENDOR spectra of these clusters in order to determine experimentally the relative sign of the apical and equatorial hyperfine values so as to determine the approach or otherwise of the electronic level overlap of the septamer to the bulk phase.

Trends. Unfortunately the EPR spectrum of the Au_7 cluster has not been observed in either inert or hydrocarbon matrices so it is not yet possible to see whether the reversal seen in the trimer clusters is repeated. Again, the lower spin density case of the copper clusters is a demonstration of the closer spacing of the 3d and 4s orbitals and similar arguments apply to the increasing spin densities as the Periodic Table is descended from lithium to potassium. It is puzzling that, as in the case of the trimeric heteronuclear alkali-metal clusters, only one heteronuclear septamer cluster is observed and there is no obvious explanation for why other septameric compositions such as Na_3K_4, *etc.*, are not also formed.

We end with the greatest puzzle of all. Why have no EPR spectra of pentameric clusters been observed other than the report by Howard *et al.*[49] of an unusual fluxional Li_5? Is there something intrinsically unstable about a cluster with five atoms, *i.e.* an inverse magic number, or is the structure of the cluster not a simple pentagon or a trigonal bipyramid but a much more puckered pseudo-planar molecule as suggested by Koutecky and co-workers[43] whose puckering frequencies have similar values to the hyperfine interactions and thus lead to line broadening beyond the detection limits of EPR spectroscopy. Most calculations on clusters predict a fairly stable pentameric structure so we as EPR spectroscopists are still left with a conundrum.

Acknowledgements

P. D. S. and A. R. Y. would like to thank the University of Wales for a Postdoctoral Research Fellowship and the Malaysian Government for a Postgraduate Research Studentship, respectively. We are grateful to Dr. Sean Howard at Cardiff for many helpful discussions on the molecular orbital calculations and the possible structures of many of the metal clusters discussed and also to Dr. Keith Preston (NRCC) for the use of his program for solving spin Hamiltonians.

References

1 H. Davies, *Phys. World*, November 1994, p. 40; A. Harthélémy, A. Fert, R. Morel and L. Steven, *Phys. World*, November 1994, p. 34; A. Henglein, *Chem. Rev.*, 1989, **89**, 1861; *Angew. Chem., Int. Ed. Engl.*, 1989, **28**.
2 E. L. Muertties and M. J. Krause, *Angew. Chem., Int. Ed. Engl.*, 1983, **22**, 135.
3 G. A. Ozin and S. Mitchell, *Angew. Chem., Int. Ed. Engl.*, 1983, **22**, 674.
4 See for example, *Faraday Symp. Chem. Soc.*, 1980, no. 14; *Faraday Discuss., R. Soc. Chem.*, 1991, **92**; *Transition Metal Clusters*, ed. B. F. G. Johnson, Wiley, New York, 1980; *Metal Clusters*, ed. M. Moskovits, Wiley, New York, 1986; *Physics and Chemistry of Small Clusters*, eds. P. Jena, B. K. Rao and S. N. Khanna, Plenum, New York, 1987; M. Morse, *Chem. Rev.*, 1986, **86**, 1049; R. Whetton, *Acc. Chem. Res.*, 1993, **26**, 49; *Small Particles of Inorganic Clusters*, eds. Olaf Echt and Edard Recknad, Springer, Berlin, 1990.
5 W. Weltner, jun., and R. J. Van Zee, *Annu. Rev. Phys. Chem.*, 1984, **35**, 291.
6 D. M. Lindsay, P. R. Herschbach and A. L. Kwiram, *Mol. Phys.*, 1976, **32**, 1199.
7 See, for example, A. M. Bass and H. P. Broida, *Formation and Trapping of Free Radicals*, Academic Press, New York, 1960; B. Mile, *Angew. Chem., Int. Ed. Engl.*, 1968, **1**, 507; *Cryochemistry*, eds. M. Moskovits and G. A. Ozin, Wiley-Interscience, New York, 1976; *Chemistry and Physics of Matrix Isolated Species*, eds. L. Andrews and M. Moskovits, Elsevier, New York, 1989.
8 (*a*) J. E. Bennett, B. Mile, A. Thomas and B. Ward, *Adv. Phys. Org. Chem.*, 1970, **8**, 1; (*b*) A. J. Buck, B. Mile and J. A. Howard, *J. Am. Chem. Soc.*, 1983, **105**, 3381; (*c*) J. A. Howard and B. Mile, *Acc. Chem. Res.*, 1987, **20**, 173.
9 L. B. Knight, jun., R. W. Woodward, R. J. Van Zee and W. Weltner, jun., *J. Chem. Phys.*, 1983, **79**, 5820.

10 R. Arratia-Perez and G. L. Malli, *J. Chem. Phys.*, 1986, **85**, 6610.
11 H. A. Jahn and E. Teller, *Proc. R. Soc. London, Ser. A*, 1937, **161**, 220.
12 See, for example, G. Fischer, *Vibronic Coupling*, Academic Press, New York, 1984; I. B. Bersuker, *The Jahn–Teller Effect and Vibronic Interactions in Modern Chemistry*, Plenum, New York, 1984.
13 *ENDOR*, eds. L. Kevan and L. D. Kispert, Wiley, New York, 1976; C. Cemerle and H. Schweiger, *Chem. Rev.*, 1991, **91**, 1481; *ENDOR Spectroscopy of Radicals in Solution: Application to Organic and Biological Chemistry*, eds. H. Kurreck, B. Kirste and W. Lubitz, VCH, Weinheim, 1988.
14 D. M. Lindsay and G. A. Thompson, *J. Chem. Phys.*, 1982, **77**, 1114; 1981, **74**, 959; G. A. Thompson, F. Tischler, D. Garland and D. M. Lindsay, *Surf. Sci.*, 1981, **106**, 408.
15 J. A. Howard, C. A. Hampson, M. Histed, H. Morris and B. Mile, *Physics and Chemistry of Small Clusters*, eds. P. Jena, B. K. Rao and S. N. Khanna, Plenum, New York, 1987, p.421.
16 D. A. Garland and D. M. Lindsay, *J. Chem. Phys.*, 1983, **78**, 2813.
17 J. A. Howard, R. Sutcliffe and B. Mile, *Chem. Phys. Lett.*, 1984, **112**, 84.
18 See, for example, J. Gaus, K. Kobe, V. Bonacic Koutecky, H. Kübling, J. Mantz, B. Reischl, S. Rutz, E. Schreiber and L. Wöste, *J. Phys. Chem.*, 1993, **97**, 12509; W. L. Cao, C. Gatti, P. J. Macdougall and R. F. W. Bader, *Chem. Phys. Lett.*, 1987, **141**, 380.
19 P. F. Meier, R. H. Hauge and J. L. Margrave, *J. Am. Chem. Soc.*, 1978, **100**, 2108.
20 S. C. Richtsmeir, M. L. Herdeweck, D. A. Dixon and J. L. Gole, *J. Phys. Chem.*, 1987, **86**, 3932.
21 G. A. Bishea, C. A. Arrington, J. M. Behm and M. D. Morse, *J. Chem. Phys.*, 1991, **95**, 8765.
22 Y. M. Hamrick, R. J. Van Zee and W. Weltner, jun., *Chem. Phys. Lett.*, 1991, **181**, 193.
23 R. J. Van Zee, D. A. Garland and W. Weltner, jun., *J. Chem. Phys.*, 1986, **84**, 5968.
24 B. Mile, C. C. Rowlands, P. D. Sillman and A. Yacob, *J. Chem. Soc., Chem. Commun.*, 1995, 775.
25 T. H. Müssig, J. R. Niklas, J. M. Spaeth and F. Granzer, *Cryst. Lattice Defects Amorph. Mater.*, 1987, **16**, 169.
26 M. Moskovits, D. P. Di Lella and K. V. Taylor, *J. Phys. Chem.*, 1983, **87**, 524.
27 G. K. Preuss, S. A. Pace and J. L. Gole, *J. Chem. Phys.*, 1970, **71**, 3553; E. A. Rohlfing and J. J. Valentini, *Chem. Phys. Lett.*, 1986, **126**, 113.
28 K. A. Gingerich, *Faraday Symp. Chem. Soc.*, 1980, no. 14, 109.
29 K. Kernisant, G. A. Thompson and D. M. Lindsay, *J. Chem. Phys.*, 1985, **82**, 4739.
30 D. M. Lindsay, G. A. Thompson and Y. Wang, *J. Am. Chem. Soc.*, 1987, **91**, 2630.
31 B. Mile, J. A. Howard, M. Histed, H. Morris and C. A. Hampson, *Faraday Discuss., R. Soc. Chem.*, 1991, **92**, 129.
32 M. D. Morse, J. B. Hopkins, P. R. R. Langridge-Smith and R. E. Smalley, *J. Chem. Phys.*, 1983, **79**, 5316; T. C. Thompson, D. G. Ruhlar and C. A. Mead, *Chem. Phys. Lett.*, 1986, **85**, 7211.
33 J. A. Howard, K. F. Preston and B. Mile, *J. Am. Chem. Soc.*, 1981, **103**, 6226; J. A. Howard, K. F. Preston, B. Mile and R. Sutcliffe, *J. Phys. Chem.*, 1983, **87**, 536; J. A. Howard, R. Sutcliffe and B. Mile, *J. Chem. Soc., Chem. Commun.*, 1983, 1449.
34 J. A. Howard, R. Sutcliffe and B. Mile, *J. Am. Chem. Soc.*, 1983, **105**, 1394.
35 E. Miyoshi, H. Tatewaki and T. Nakamura, *J. Chem. Phys.*, 1983, **78**, 815; S. P. Walch and B. C. Laskowski, *J. Chem. Phys.*, 1986, **84**, 2734; J. R. Langhoff, C. W. Bauschlicher, jun., S. P. Walch and B. C. Laskowski, *J. Chem. Phys.*, 1986, **85**, 7211.
36 G. A. Bishea and M. D. Morse, *J. Chem. Phys.*, 1991, **95**, 5646.
37 S. B. H. Bach, D. A. Garland, R. J. Van Zee and W. Weltner, jun., *J. Chem. Phys.*, 1987, **87**, 869.
38 R. J. Van Zee and W. Weltner, jun., *J. Chem. Phys.*, 1990, **92**, 6976.
39 G. A. Thompson, F. Tischler and D. M. Lindsay, *J. Chem. Phys.*, 1983, **78**, 5946.
40 D. A. Garland and D. M. Lindsay, *J. Chem. Phys.*, 1984, **80**, 4761.
41 P. Fantucci, J. Koutecky and G. Pacchioni, *J. Chem. Phys.*, 1984, **80**, 325.
42 J. Demuyack and Aa. Veillard, *Faraday Symp. Chem. Soc.*, 1980, **14**, 170.
43 G. Pacchioni, D. Plavsic and J. Koutecky, *Ber. Bunsenges. Phys. Chem.*, 1983, **87**, 503.
44 S. W. Wang, *J. Chem. Phys.*, 1985, **82**, 4633.
45 V. Bonacic Koutecky, P. Fantucci and J. Koutecky, *Chem. Rev.*, 1991, **91**, 1035.
46 M. R. Hoare and P. Pale, *Nature Phys. Sci.*, 1972, **35**, 236; *Adv. Chem. Phys.*, 1971, **40**, 49; S. Ino, *J. Phys. Soc. Jpn.*, 1966, **21**, 346; R. Monot, *Physical Latent Image Formation of Silver Halides*, ed. A. Balderschi, World Science, Singapore, 1984, p. 175.
47 B. Mile, P. D. Sillman, C. C. Rowlands and A. R. Yacob, *Chem. Phys. Lett.*, 1995, **236**, 603.
48 R. N. Edmonds, M. R. Harrison and P. P. Edwards, *Annu. Rep. Prog. Chem., Sect. C*, 1985, **82**, 266.
49 J. A. Howard, H. A. Joly, R. Jones, P. P. Edwards, R. J. Singer and D. E. Logan, *Chem. Phys. Lett.*, 1993, **204**, 128.

Received 26*th July* 1995; *Paper* 5/06725A